Ref.TH.1436-CERN

POLARIZATION RELATIONS IN CHARGE AND HYPERCHARGE EXCHANGE REACTIONS

A.D. Martin, C. Michael
CERN - Geneva

and

R.J.N. Phillips
Rutherford Laboratory, Berkshire

A B S T R A C T

Relations between polarizations in charge and hypercharge exchange reactions are derived. The idea is that K^*_{890} and K^{**}_{1400} exchange, including unspecified absorptive corrections, are related to ρ and A_2 exchanges by SU(3) octet symmetry, with a scale factor to represent symmetry breaking between the ρ-A_2 and the K^*-K^{**} trajectories. This hypothesis is consistent with the present data on $\bar{K}N \to \pi\Sigma(\pi\Lambda)$ and $\pi N \to K\Sigma(K\Lambda)$. It leads to simple relations between the polarized cross-sections $P\,d\sigma/dt$, relating the above reactions to $K^-p \to \bar{K}^0n$, $K^+n \to K^0p$, $\pi^-p \to \pi^0n$, $\pi^-p \to \eta^0n$. Predictions are made, on this basis, for polarization in $K^-p \to \bar{K}^0n$, $K^+n \to K^0p$ and $\pi^-p \to \eta^0n$ at 4 GeV/c, and for $K^-p \to \bar{K}^0n$ at 7 GeV/c. Finally, some supplementary conjectures lead to predictions about polarization in baryon-baryon and baryon-antibaryon reactions, $np \to pn$, $\bar{p}p \to \bar{n}n$, $\bar{p}p \to \bar{\Lambda}\Lambda$, etc., and also in $K^0_Lp \to K^0_Sp$ regeneration.

Ref.TH.1436-CERN
7 December 1971

1. - INTRODUCTION

We study vector and tensor meson exchange processes such as charge exchange (CEX) and hypercharge exchange meson baryon scattering. Although a model independent analysis [1] of ρ exchange in πN charge exchange exists at 6 GeV/c, in general the amplitude structure of vector and tensor exchange is not reliably known. We apply SU(3) symmetry relations to the t channel exchanges and are able to correlate and predict data without invoking specific models for exchange amplitudes.

Evidence for the dominance of octet exchange in charge and hypercharge exchange reactions comes from the success of the Barger-Cline sum rule [2] for charge exchange cross-sections, and from the suppression of $I = \frac{3}{2}$ exchanges in $\bar{K}N \to \pi\Sigma$ and $\pi N \to K\Sigma$ as shown [3] by measurements of the double charge exchange reactions and by comparison of reactions with different charge states. Furthermore, the structure of the polarizations in the pair of line reversed reactions $\pi^- p \to K^0\Lambda$ and $K^- p \to \pi^0\Lambda$ closely resemble the polarizations in the pair $\pi^+ p \to K^+\Sigma^+$ and $K^- p \to \pi^-\Sigma^+$. A plausible explanation [4] is that the vector and tensor exchanges in these reactions are related by SU(3) octet symmetry with common F/D ratios. This is to be expected, if we start with exchange-degenerate (EXD) K^* and K^{**} poles, belonging to octets. Then a multiplicative modification of these poles by an SU(3) singlet will preserve octet dominance. The resulting cuts have sufficient freedom to accommodate the non-zero polarizations and unequal line reversed cross-sections. Thus we take over from duality diagrams the expectation that the structure of the amplitudes in the three "real" processes $K^+ n \to K^0 p$, $K^- p \to \pi^-\Sigma^+$ and $K^- p \to \pi^0\Lambda$ are similar, likewise for the three "rotating" processes $K^- p \to \bar{K}^0 n$, $\pi^+ p \to K^+\Sigma^+$, $\pi^- p \to K^0\Lambda^0$.

An example of a multiplicative SU(3) singlet modification of EXD poles is absorption by a Pomeron *). We present the expectations of such models which will allow the assumptions to be checked, and thus possible non-singlet modifications of the poles (such as Regge-Regge cut effects, s channel effects, etc.) to be identified.

---

*) We need retain only the feature that the resultant amplitudes are proportional in strength to the pole amplitudes for reactions with similar structure.

Consider now the symmetry breaking arising from the $K^* - K^{**}$ trajectory lying $\Delta\alpha \approx 0.2$ below the $\rho - A_2$ trajectory. In a Regge pole model this gives rise to an over-all symmetry breaking factor $\lambda^{-1} = (-is/s_o)^{\Delta\alpha}$ which, for $s > s_o$, enhances the $\rho - A_2$ exchange amplitudes relative to the $K^* - K^{**}$ exchange amplitudes. λ is thus independent of t and is the same for non-flip and flip amplitudes. Although λ is complex only $|\lambda|^2$ enters experimental observables. We note that the shifting of nonsense wrong signature zeros is neglected *). The latter effect could have been included by comparing data at fixed α - but the known modification of the pole t dependence by absorption makes this untenable.

To achieve a description of the combined charge and hypercharge reactions we first determine $|\lambda|$ from the forward data and then assume that it is constant in t. In a dual model the size of s_o is fixed by $1/\alpha'$ and the empirical value of λ is found to be consistent with the estimate using this s_o and $\Delta\alpha \approx 0.2$. In Section 4, we return to the experimental evidence for a possible t dependence of λ.

2. - SU(3) RELATIONS

With the above hypothesis the s channel non-flip and flip amplitudes, $f_\pm$, have the structure listed in Table I. Here V and T denote the vector (ρ or K^*) and tensor (A_2 or K^{**}) exchange contributions respectively, normalized to those for KN charge-exchange. The flip and non-flip F/D ratios are found to be $F_- \approx 1/4$ and $F_+ \approx 3/2$, and so we see from the Table that the flip/non-flip amplitude ratio is $1 : 3/8 : -1/4$ for $K^+n \to K^0p$: : $K^-p \to \pi^0\Lambda$: $K^-p \to \pi^-\Sigma^+$, and similarly for the three "rotating" processes.

---

*) In fact, for all the hypercharge exchanges that we consider (except η, η' production) there are no NWSZ : exchange-degenerate pairs of Regge poles are as well related by factors $\sim(-is/s_o)^{\Delta\alpha}$ as by comparison at the same α.

The phases of $V_\pm$, $T_\pm$ include general multiplicative corrections and are not assumed to be those of the exchange degenerate pole model. Thus line-reversed cross-sections can be unequal, and, since $\rho - A_2$ exchange in KN CEX has relatively more flip than in the $K^* - K^{**}$ exchange processes, the apparent line reversal inequality will be less for the former case if the flip amplitudes have phases closer to pole expectations.

Some consequences of Table I may be summarized. First there are linear relations among the amplitudes which will lead to triangular inequalities

$$2\lambda\, f(K^+n \to K^0p) = \sqrt{12}\, f(K^-p \to \pi^0\Lambda) + f(K^-p \to \pi^-\Sigma^+) \tag{1}$$

$$2\lambda\, f(K^-p \to \bar{K}^0n) = \sqrt{6}\, f(\pi^-p \to K^0\Lambda) - f(\pi^+p \to K^+\Sigma^+). \tag{2}$$

Then, one has the Barger-Cline sum rule [2] for $d\sigma/dt$ and its analogue [5] for $Pd\sigma/dt$

$$\frac{d\sigma}{dt}(\pi^-p \to \pi^0n) + 3\frac{d\sigma}{dt}(\pi^-p \to \eta_8 n) = \frac{d\sigma}{dt}(K^-p \to \bar{K}^0n) + \frac{d\sigma}{dt}(K^+n \to K^0p) \tag{3}$$

$$P\frac{d\sigma}{dt}(\pi^-p \to \pi^0n) + 3P\frac{d\sigma}{dt}(\pi^-p \to \eta_8 n) = P\frac{d\sigma}{dt}(K^-p \to \bar{K}^0n) + P\frac{d\sigma}{dt}(K^+n \to K^0p) \tag{4}$$

and hyperon production sum rules relating η_8 and η_1. For example for Λ production we have

$$\frac{d\sigma}{dt}(K^-p \to \eta_8\Lambda) + \frac{2}{S_T^2}\frac{d\sigma}{dt}(K^-p \to \eta_1\Lambda) = \frac{d\sigma}{dt}(K^-p \to \pi^0\Lambda) + \frac{d\sigma}{dt}(\pi^-p \to K^0\Lambda) \tag{5}$$

where S_T^2 is the cross-section ratio $\sigma(\pi^-p \to \eta_1 n)/(\pi^-p \to \eta_8 n)$. For simplicity we present the relation in terms of the pure SU(3) states η_1, η_8. The relation for the physical states η and η' (or X^0) follows immediately on specifying the $\eta - \eta'$ mixing angle [6].

Further, as we have made the EXD assumption that the vector and tensor exchanges have the same F/D ratio, F_+, we relate the line-reversal breaking at $t = 0$ for the three pairs of processes :

$$\frac{\frac{d\sigma}{dt}(K^+n\to K^0p)}{\frac{d\sigma}{dt}(K^-p\to \bar{K}^0n)} = \frac{2\frac{d\sigma}{dt}(K^-p\to\pi^0\Lambda)}{\frac{d\sigma}{dt}(\pi^-p\to K^0\Lambda)} = \frac{\frac{d\sigma}{dt}(K^-p\to\pi^-\Sigma^+)}{\frac{d\sigma}{dt}(\pi^+p\to K^+\Sigma^+)} \qquad (6)$$

at $t = 0$.

Consider now relations involving the polarizations. We will use the notation

$$P\frac{d\sigma}{dt} = 2\,\mathrm{Im}(f_+f_-^*) = 2|f_+||f_-|\sin\phi_{+-} \qquad (7)$$

The relative phase, $\phi_{+-}(t)$, between f_+ and f_- can be seen to be common to the three "real" processes and common to the three "rotating" processes. This phase is also an exchange degeneracy breaking effect and we study the consequences of ascribing it to unitary singlet absorption rather than Regge-Regge cut effects or s channel effects. In general, in an effective octet exchange model, one might allow F_+, F_- and λ to vary with t and to be different for the "real" and "rotating" amplitudes. We return to this possibility in Section 4. However, assuming $F_\pm$ and λ are independent of t, we may relate the t dependences of $Pd\sigma/dt$ *) as follows :

$$P\frac{d\sigma}{dt}(K^-p\to\bar{K}^0n) = C_\Lambda P\frac{d\sigma}{dt}(\pi^-p\to K^0\Lambda) = C_\Sigma P\frac{d\sigma}{dt}(\pi^+p\to K^+\Sigma^+)$$
$$P\frac{d\sigma}{dt}(K^+n\to K^0p) = 2C_\Lambda P\frac{d\sigma}{dt}(K^-p\to\pi^0\Lambda) = C_\Sigma P\frac{d\sigma}{dt}(K^-p\to\pi^-\Sigma^+) \qquad (8)$$

where the constants are given by

$$C_\Lambda = \frac{6}{|\lambda|^2(2F_+ + 1)(2F_- + 1)}, \qquad C_\Sigma = \frac{1}{|\lambda|^2(2F_+ - 1)(2F_- - 1)}. \qquad (9)$$

---

*) Similar relations hold for $X(d\sigma/dt) = 2\mathrm{Re}(f_+f_-^*) = (R\cos\theta_P + A\sin\theta_P)d\sigma/dt$.

Similarly for the η production processes we have

$$P\frac{d\sigma}{dt}(K^-p\to\bar{K}^0n)+P\frac{d\sigma}{dt}(\pi^-p\to\pi^0n)-P\frac{d\sigma}{dt}(\pi^-p\to\eta_8 n)$$

$$=2C_\Lambda P\frac{d\sigma}{dt}(K^-p\to\eta_8\Lambda)=2C_\Sigma P\frac{d\sigma}{dt}(K^-n\to\eta_8\Sigma^-),$$

$$P\frac{d\sigma}{dt}(\pi^-p\to\eta_1 n)=C_\Lambda P\frac{d\sigma}{dt}(K^-p\to\eta_1\Lambda)=C_\Sigma P\frac{d\sigma}{dt}(K^-n\to\eta_1\Sigma^-).$$

3. - DATA AND PREDICTIONS

Consider the first six reactions of Table I. To study the above SU(3) relations we require data for the three "real" (or the three "rotating") processes at the same energy. The highest suitable momenta at which sufficient data exist for the "real" processes is in the region of 4 GeV/c. However, data exist so that the "rotating" processes can be studied at 7 GeV/c as well as at 4 GeV/c.

The data in the region of 4 GeV/c are shown on Figs. 1 and 2 together with interpolating curves. As neither the $K^-p\to\bar{K}^0n$ nor the $K^+n\to K^0p$ polarization has yet been measured, we show instead on the figures the prediction obtained as described below. (In general we show predictions by dashed lines and interpolations through data points by continuous lines.) Figure 3 contains the available data at 7 GeV/c - the $\pi^-p\to K^0\Lambda$ curve is calculated from the $\pi^+p\to K^+\Sigma^+$ 7 GeV/c data [7a] using the observed $\pi^-p\to K^0\Lambda/\pi^-p\to K^0\Sigma^0$ differential cross-section ratio [7c] at 8 GeV/c.

First we determine the F/D ratio for the non-flip amplitudes, F_+, and the symmetry breaking factor λ by comparing the cross-sections at $t = 0$

$$\left.\frac{d\sigma(\Sigma)/dt}{d\sigma(\Lambda)/dt}\right|_0 = 6\left(\frac{2F_+ - 1}{2F_+ + 1}\right)^2, \qquad \left.\frac{d\sigma(\Sigma)/dt}{d\sigma(K)/dt}\right|_0 = |\lambda|^2 (2F_+ - 1)^2.$$

When the $K^- p \to \pi^0 \Lambda$ data is used the factor of 6 is replaced by 12 in the first equation. To reduce the uncertainty in extrapolating the differential cross-sections to $t = 0$ we also plotted $\ell n\, d\sigma/dt|_0$ versus $\ell n\, p_L$ using data at all available lab. momenta p_L. This is particularly relevant for $\pi^+ p \to K^+ \Sigma^+$ at 4 GeV/c since very accurate forward data at 3, 5, 7 GeV/c have recently been obtained [7b]. The forward $d\sigma/dt$ that are used are listed in Table II together with the resulting values of F_+ and $|\lambda|^2$. The values listed for $\Delta\alpha$, obtained from $|1/\lambda| = (s/s_0)^{\Delta\alpha}$ with $s_0 = 1\ \text{GeV}^{-2}$, compare well with the expectations of parallel $\rho - A_2$ and $K^* - K^{**}$ trajectories : $\Delta\alpha = \alpha'(m_\rho^2 - m_{K^*}^2) \approx 0.2$.

By comparing $P\, d\sigma/dt$ for the line-reversed hypercharge exchange reactions we find from Eqs. (8) that C_Λ / C_Σ is independent of t to within the experimental errors. This ratio, together with the underlying assumption that $F_\pm$ and λ are independent of t leads to the estimate of the flip F/D ratio, F_-, listed in Table II.

If the hypothesis of Section 2 is correct, all the predictions for $F_\pm$ should be the same. Further the two (line-reversed) predictions for C_Λ / C_Σ and $|\lambda|^2$ at 4 GeV/c should be equal. Present data are consistent with such assumptions.

From a knowledge of $F_\pm$ and $|\lambda|^2$ we can use Eqs. (8) to predict the KN CEX polarizations from either the Λ or the Σ production data. The dashed polarization curves shown in Figs. 1 and 2 with representative errors, are the results of averaging the predictions from the P_Λ and P_Σ data. The 7 GeV/c $K^- p \to \bar{K}^0 n$ polarization in Fig. 3 is calculated from the data for P_Σ using the average value of the flip F/D ratio found at 4 GeV/c, namely $F_- = 0.27$.

Consider now the predictions for $\pi^- p \to \eta n$. First we check the SU(3) sum rule, Eq. (3), at 4 GeV/c using the interpolated $\pi^- p \to \pi^0 n$ data shown in Fig. 4 together with the KN CEX data interpolations of Figs. 1 and 2. In Fig. 4, the resulting η cross-section is compared with

data at nearby energies. Further from the πN CEX polarization data (the average at 4 GeV/c is plotted in Fig. 4), we use Eqs. (4) and (8) to predict the $\pi^- p \to \eta n$ polarization from the hypercharge exchange data. The result, also given in Fig. 4, is positive for $-t < 1$ GeV^2 and may be compared with the value $P = 0.27 \pm 0.14$ for $0.11 < -t < 0.26$ measured by Drobnis et al. [13d] at 3.47 GeV/c.

3.1. - $K_L^o p \to K_S^o p$ regeneration

Both SU(3) singlet and octet vector exchanges may contribute to this process. Exchange degeneracy supports the quark model prediction that the ϕ meson decouples from $\bar{p}p$, so that ω and ϱ exchanges remain. Assuming that these contributions are related by SU(3) yields an amplitude $-(2F-1)V$ for $K_L^o p \to K_S^o p$ relative to the amplitudes listed in Table I. Using the previously obtained F/D ratios ($F_+ \approx 1.42$, $F_- \approx 0.27$) we may relate the polarization to that in $\pi^- p \to \pi^o n$

$$P \frac{d\sigma}{dt}(K_L^o p \to K_S^o p) = \frac{1}{2}(2F_+ - 1)(2F_- - 1) P \frac{d\sigma}{dt}(\pi^- p \to \pi^o n). \qquad (10)$$

Furthermore, since a decomposition into s channel helicity flip and non-flip amplitudes $f_\pm$ exists [1] for $\pi^- p \to \pi^o n$ at 6 GeV/c, we may predict the regeneration cross-section

$$\frac{d\sigma}{dt}(K_L^o p \to K_S^o p) = \frac{1}{2}(2F_+ - 1)^2 |f_+|^2 + \frac{1}{2}(2F_- - 1)^2 |f_-|^2.$$

The predictions are shown in Fig. 4 together with the regeneration cross-section data [14] from a 4 to 8 GeV/c K^o spectrum which is weighted near 5 GeV/c at small t and below 5 GeV/c for larger t. More accurate regeneration data would enable the ω spin flip component to be better determined.

3.2. - Baryon-baryon and baryon-antibaryon scattering

Similarly ϱ, A_2, K^*, K^{**} exchanges occur in $\bar{p}p \to \bar{n}n$, $\bar{p}p \to \bar{\Lambda}\Lambda$, $\bar{p}p \to \bar{\Sigma}\Sigma$, $\bar{\Sigma}\Lambda$ and the crossed reactions $np \to pn$, $\Lambda p \to p\Lambda$, $\Sigma p \to p\Sigma$, $p\Lambda$. The last three are inaccessible at present but may eventually be measured with hyperon beams.

Let us consider only these vector and tensor exchange contributions ; this is a strong assumption, since (in charge exchange) it means neglecting one-pion exchange, known to be important at very small t. Then each helicity amplitude in baryon-baryon scattering has the general form $(T - V)$, and the corresponding baryon-antibaryon term has the form $(T + V)$. Different reactions are related by the F_+ and F_- ratios of the Regge pole couplings, presumably shared by the absorptive corrections. In the present case, however, it appears that we cannot usefully exploit these ratios.

In general *), there are six independent s channel helicity amplitudes $f_1 = f(++,++)$, $f_2 = f(++,--)$, $f_3 = f(+-,+-)$, $f_4 = f(+-,-+)$, $f_5 = f(++,+-)$, $f_6 = f(+-,++)$, where $\pm$ denotes helicity $\pm 1/2$. Polarization is given by

$$P\frac{d\sigma}{dt} = \mathrm{Im}\left[(f_1+f_2)f_6^* - (f_3-f_4)f_5^*\right] \qquad (11)$$

with a suitable normalization for the f_i. Since f_1 and f_3 are non-flip at both vertices, they have a common transformation property between different reactions, governed by the non-flip F/D ratio. Since f_2 and f_4 are flip at both vertices, their transformations are governed by F_- instead. Hence $Pd\sigma/dt$ has two independent components, and the different reactions are not simply related by constant factors, unlike the meson-baryon case.

Further simplifying assumptions suggest themselves, however. If the basic Regge poles are exchange-degenerate, polarization comes from interference with cuts. For natural parity exchange $f_1 = f_3$, $f_4 = -f_2$, $f_5 = -f_6$ to leading order in s. Now f_1 and f_5 are amplitudes with net helicity flip $n = 0$ and $n = 1$ respectively and, as their parity relations are maintained in the presence of cuts, Eq. (11) becomes

---

*) For $\bar{p}p \to \bar{n}n$ and $np \to pn$ there are only five independent amplitudes since C invariance and isospin conservation require that $f_5 = -f_6$.

$$P \frac{d\sigma}{dt} \approx Im\left[f(n=0)\, f^{*}(n=1) \right] \qquad (12)$$

We have assumed that f_4 and f_2 are negligible for small t. It is now tempting to assume that the net $n = 0$ and $n = 1$ baryon-baryon amplitudes above are similar - and in fact roughly proportional to - the $n = 0, 1$ meson-baryon terms. Then $Pd\sigma/dt$ for the baryon-antibaryon cases $\bar{p}p \to \bar{n}n$, $\bar{p}p \to \bar{\Lambda}\Lambda$, $\bar{p}p \to \bar{\Sigma}\Sigma$ are simply proportional to $Im(T+V)_{+}\,(T+V)^{*}_{-}$ and will have the same structure as $Pd\sigma/dt$ for $K^{-}p \to \bar{K}^{o}n$, $\pi^{-}p \to K^{o}\Lambda$, $\pi^{+}p \to K^{+}\Sigma^{+}$ respectively. In the same way $Pd\sigma/dt$ for the baryon-baryon processes $np \to pn$, $\Lambda p \to p\Lambda$, $\Sigma p \to p\Sigma$ are similar to those for $K^{+}n \to K^{o}p$, $K^{-}p \to \pi^{o}\Lambda$, $K^{-}p \to \pi^{-}\Sigma^{+}$ respectively. Experimental polarization data for $np \to pn$ [15] show the same sign *) and structure as our $K^{+}n \to K^{o}p$ predictions ; for $\bar{p}p \to \bar{\Lambda}\Lambda$ and $\bar{p}p \to \bar{\Sigma}\Sigma$ the data [16),17] also show Λ and Σ polarizations similar to those in $\pi N \to K\Lambda$ and $K\Sigma$ as noted by Plaut [18].

4. - ANALYSIS OF SU(3) BREAKING

We wish to investigate the magnitude, s dependence and t dependence of the symmetry breaking factor λ to see if it checks with our assumption of a $(-is/s_o)^{-\Delta\alpha}$ behaviour. This can be accomplished by considering the triangular inequalities that follow from the amplitude relations of Eqs. (1) and (2). These relations assume only dominance of SU(3) octet exchange. Thus, independent of any choice of the F/D ratios, we have at each t value

$$\left(\sqrt{\sigma_\Lambda} - \sqrt{\sigma_\Sigma}\right)^2 \leq |\lambda|^2 \sigma_K \leq \left(\sqrt{\sigma_\Lambda} + \sqrt{\sigma_\Sigma}\right)^2 \qquad (13)$$

---

*) The data of Ref. 15) use a different sign convention for polarization in np charge exchange.

$$\left(\sqrt{(1\pm P_\Lambda)\sigma_\Lambda} - \sqrt{(1\pm P_\Sigma)\sigma_\Sigma}\right)^2 \leq |\lambda|^2(1\pm P_K)\sigma_K \leq \left(\sqrt{(1\pm P_\Lambda)\sigma_\Lambda} + \sqrt{(1\pm P_\Sigma)\sigma_\Sigma}\right)^2 \tag{14}$$

where σ_K, σ_Σ, σ_Λ denote $4d\sigma(K)/dt$, $d\sigma(\Sigma)/dt$, (6 or 12) $d\sigma(\Lambda)/dt$ respectively. The notation is that of Table II ; the factor 6 (12) is to be used if the equalities are applied to the "rotating" ("real") reactions.

These relations may be cast into bounds for $|\lambda(t)|^2$. These are shown in Fig. 5. The dashed lines are the bounds resulting from Eq. (13) using the differential cross-section data only, and the solid lines follow from the polarized cross-section inequalities, Eq. (14), upon adding the relations $(1 \pm P_K)\sigma_K$ to eliminate the unmeasured KN CEX polarization, P_K. This latter bound is stronger since when $P_\Lambda \neq P_\Sigma$ the cross-section bound cannot be saturated.

Our underlying SU(3) assumption implies that the Λ and Σ production amplitudes are relatively real. In Section 3, we used the observed ratio of the moduli of these amplitudes to solve for F/D. We found two solutions which correspond to 0° and 180° relative phases. The F/D solution of Table II was selected on physical grounds and corresponds to 0° relative phase in the Λ, Σ non-flip amplitudes, f_+, and to 180° in f_-. Thus $|\lambda(t)|^2$ should be near its lower bound when f_+ dominates (for example at $t = 0$) and near its upper bound if f_- dominates. A constant value of λ shows, at small t, the expected tendency of an increasing amount of spin-flip as $-t$ increases, but beyond $-t \approx 0.5$ GeV^2 there is evidence for a need of a t dependence of λ.

If λ does vary with t, then we can still bound the KN CEX polarizations by optimization [19] of the triangular inequalities for general λ. The resulting polarization bounds, which depend only on octet exchange dominance, are shown in Fig. 6, together with the bounds which would apply if λ were independent of t [that is $\lambda(t) = \lambda(0)$]. Regardless of the t dependence of the F/D ratios $F_\pm$ these latter bounds are expected to be relevant for small t since we know in this t region that $\lambda(t)$ is near its lower bound.

5. - SUMMARY

We have investigated the predictions for a general class of t channel models inspired by SU(3) and duality. Present data are consistent with this approach. Moreover the resulting non-flip and flip F/D ratios are consistent with other determinations [20] and the magnitude of the symmetry breaking factor λ agrees with dual model estimates based on the mass differences of the exchanged mesons.

Polarization for charge exchange processes at or above 4 GeV/c will allow a direct check of the region of validity of this approach. Possible Regge-Regge cut or s channel effects might be necessary at lower energies and may thus be illuminated.

Process	f
$K^+n \to K^0p$	$(T - V)$
$K^-p \to \pi^0\Lambda$	$\frac{\lambda}{\sqrt{12}}(2F + 1)(T - V)$
$K^-p \to \pi^-\Sigma^+$	$-\lambda(2F - 1)(T - V)$
$K^-p \to \bar{K}^0n$	$-(T + V)$
$\pi^-p \to K^0\Lambda$	$-\frac{\lambda}{\sqrt{6}}(2F + 1)(T + V)$
$\pi^+p \to K^+\Sigma^+$	$-\lambda(2F - 1)(T + V)$
$\pi^-p \to \pi^0n$	$-\sqrt{2}$ V
$\pi^-p \to \eta_8 n$	$\sqrt{\frac{2}{3}}$ T
$\pi^-p \to \eta_1 n$	$\sqrt{\frac{2}{3}}\, S_T$ T
$K^-p \to \eta_8\Lambda$	$-\frac{\lambda}{6}(2F + 1)(T + 3V)$
$K^-p \to \eta_1\Lambda$	$+\frac{\lambda}{3}(2F + 1)\, S_T$ T
$K^-n \to \eta_8\Sigma^-$	$-\frac{\lambda}{\sqrt{6}}(2F - 1)(T + 3V)$
$K^-n \to \eta_1\Sigma^-$	$\sqrt{\frac{2}{3}}\lambda(2F - 1)\, S_T$ T

TABLE I Composition of the amplitudes, $f_\pm$, using SU(3) octet exchange. V and T denote vector (ϱ or K^*) and tensor (A_2 or K^{**}) exchanges respectively, and are taken to have the equal F/D ratios as predicted by EXD. λ is the SU(3) breaking factor arising from the difference of the ϱ, A_2 and the K^*, K^{**} trajectories. S_T fixes the singlet/octet ratio of η couplings as defined in Ref. 6). F is the fraction of F type VBB coupling defined so that F + D = 1. For convenience we have omitted the $\pm$ subscripts from $f_\pm$, $V_\pm$, $T_\pm$, $F_\pm$ which distinguish non-flip and flip amplitudes

	"Real" processes $K \equiv K^+n \to K^0p$ $\Lambda \equiv K^-p \to \pi^0\Lambda$ $\Sigma \equiv K^-p \to \pi^-\Sigma^+$	"Rotating" processes $K \equiv K^-p \to \bar{K}^0n$ $\Lambda \equiv \pi^-p \to K^0\Lambda$ $\Sigma \equiv \pi^+p \to K^+\Sigma^+$	
	4 GeV/c	4 GeV/c	7 GeV/c
$\left.\frac{d\sigma/dt\ (\Sigma)}{d\sigma/dt\ (\Lambda)}\right\|_0$	$\frac{0.68 \pm 0.13}{0.24 \pm 0.06}$	$\frac{0.58 \pm 0.1}{0.43 \pm 0.1}$	$\frac{0.30 \pm 0.05}{0.168 \pm 0.04}$
F_+	1.44	1.40	1.70
$\left.\frac{d\sigma/dt\ (\Sigma)}{d\sigma/dt\ (K)}\right\|_0$	$\frac{0.68 \pm 0.13}{0.76 \pm 0.16}$	$\frac{0.58 \pm 0.1}{0.56 \pm 0.08}$	$\frac{0.30 \pm 0.05}{0.233 \pm 0.03}$
$\|\lambda\|^2$	0.25	0.32	0.22
$\Delta\alpha$	0.32	0.26	0.28
C_Λ / C_Σ	3.7 / (-6.4)	3.4 / (-3.1)	No P_Λ data
F_-	0.33	0.22	-

TABLE II The non-flip and flip F/D ratios, $F_\pm$, and the symmetry breaking factor $|\lambda|^2$ calculated from the data. The forward differential cross-sections are given in mb.GeV^{-2}. The forward Σ/Λ ratio gives two solutions for F_+ but only the physically acceptable one is shown (see Section 4). The value for C_Λ / C_Σ is calculated by suitably averaging the polarized cross-section ratio in the interval $0 < -t < 0.7$ GeV^2.

REFERENCES

1) F. Halzen and C. Michael - Phys.Letters 36B, 367 (1971).

2) V. Barger and D. Cline - Phys.Rev. 156, 1522 (1967).

3) F. Halzen, J. Mandula, J. Weyers and G. Zweig - CERN Preprint TH. 1371 (1971) ;
C.W. Akerlof et al. - Phys.Rev.Letters 27, 539 (1971).

4) A.C. Irving, A.D. Martin and C. Michael - Nuclear Phys. B32, 1 (1971).

5) A. Krzywicki - Proceedings of the Vth Rencontres de Moriond (1970).

6) A.D. Martin and C. Michael - CERN Preprint TH. 1427 (1971).

7) [$\pi N \to K\Sigma$]
a) S.M. Pruss et al. - Phys.Rev.Letters 23, 189 (1969) ;
b) P. Kalbaci et al. - Phys.Rev.Letters 27, 74 (1971).

8) [$\pi N \to K\Lambda$]
a) M. Abramovich et al. - Nuclear Phys. B22, 477 (1971) ;
b) O.I. Dahl et al. - Phys.Rev. 163, 1430 (1967) ;
c) S. Ozaki et al. - B.N.L. Preprint (1970).

9) [$\bar{K}N$ CEX]
a) L. Moscoso et al. - Phys.Letters 32B, 513 (1970) ;
b) M. Aguilar-Benitez et al. - B.N.L. Preprint 15900 (1971) ;
c) Amsterdam-Nijmegen Collaboration - Submitted to Lund Conference (1969) ;
d) P. Astbury et al. - Phys.Letters 23, 396 (1966).

10) [$\bar{K}N \to \pi\Sigma, \pi\Lambda$]
a) D.J. Crennell et al. - Phys.Rev.Letters 23, 1347 (1969) ;
b) L. Moscoso et al. - Saclay-Ecole Polytechnique Preprint (1971) ;
c) J.S. Loos et al. - Phys.Rev. 173, 1330 (1968) ;
d) Amsterdam-Nijmegen Collaboration - Private communication and submitted to Amsterdam Conference (1971) ;
e) W.L. Yen et al. - Phys.Rev. 188, 2011 (1969).

11) [$\bar{K}N$ CEX]
a) Y. Goldschmidt-Clermont et al. - Phys.Letters 27B, 602 (1968) ;
b) D. Cline et al. - Nuclear Phys. B22, 247 (1970).

12) [πN CEX]
a) G. Giacomelli, P. Pini and S. Stagni - CERN-HERA 69-1 (1969) ;
b) O. Guisan - Proceedings of the VIth Rencontres de Moriond (1971), J. Tran Thanh Van, Editor ; see also Ref. 1).

13) [$\pi^- p \to \eta n$]
a) E.H. Harvey et al. - Phys.Rev.Letters 27, 885 (1971) ;
b) P. Borgeaud - Saclay report CEA-R-4037 (1970) ;
c) J. Hladky et al. - Phys.Letters 31B, 475 (1970) ;
d) D.D. Drobnis et al. - Phys.Rev.Letters 20, 274 (1968).

14) [$K_L p \to K_S p$]
A.D. Brody et al. - Phys.Rev.Letters 26, 1050 (1971).

15) [$\bar{p}p \to \bar{\Lambda}\Lambda$]
H.W. Atherton et al. - Nuclear Phys. B29, 477 (1971).

16) [$\bar{p}p \to \bar{\Sigma}\Sigma$]
H.W. Atherton et al. - CERN Preprint D.Ph.II/PHYS 71-29 (1971).

17) [$np \to pn$]
P.R. Robrish et al. - Phys.Letters 31B, 617 (1970).

18) G. Plaut - Nuclear Phys. B35, 221 (1971).

19) G.V. Dass and J. Froyland - CERN Preprint TH. 1435 (1971).

20) G. Ebel et al. - Nuclear Phys. B33, 317 (1971).

FIGURE CAPTIONS

Figure 1 Differential cross-sections and polarizations near 4 GeV/c for the three "rotating" reactions. $d\sigma/dt$ data for $\pi N \to K\Sigma$ (4 GeV/c [7a,b]) ; $\pi N \to K\Lambda$ (3.9 GeV/c [8a] and 4 GeV/c [8b]) and $K^-p \to \bar{K}^0 n$ (3.9 GeV/c [9a], 3.95 GeV/c [9b] and 4.2 GeV/c [9c]) are shown together with interpolating curves at 4 GeV/c. Polarization data for $\pi N \to K\Sigma$ at 4 GeV/c [7a], $\pi N \to K\Lambda$ at 3.9 GeV/c [8a] and interpolating curves are shown. Using these interpolations, we predict (as described in Section 3) the $K^-p \to \bar{K}^0 n$ polarization shown by the dashed curve with representative errors.

Figure 2 Differential cross-sections and polarizations near 4 GeV/c for the three "real" reactions. $d\sigma/dt$ data for $\bar{K}N \to \pi\Sigma$ (3.95 GeV/c [10b] and 4.07 GeV/c [10c]) ; $\bar{K}N \to \pi\Lambda$ (3.9 GeV/c [10a], 3.95 GeV/c [10b] and 4.2 GeV/c [10d]) and $K^+n \to K^0p$ (3 GeV/c [11a] and 5.5 GeV/c [11b]) are shown together with interpolating curves at 4 GeV/c. Polarization data for $\bar{K}N \to \pi\Sigma$ (3.95 GeV/c [10b] and 4.2 GeV/c [10d] combined), $\bar{K}N \to \pi\Lambda$ (3.9 GeV/c [10a], 3.95 GeV/c [10b], 4.2 GeV/c [10d] and 4.5 GeV/c [10e] combined) and interpolating curves are shown. Using these interpolations, we predict the $K^+n \to K^0p$ polarization shown by the dashed curve with representative errors.

Figure 3 The three "rotating" reactions near 7 GeV/c. $\pi^+p \to K^+\Sigma^+$ $d\sigma/dt$ and P data at 7 GeV/c [7a,b], $K^-p \to \bar{K}^0 n$ $d\sigma/dt$ data at 7.1 GeV/c [9a] and interpolations are shown. The $\pi^-p \to K^0\Lambda$ differential cross-section (shown dashed) is determined from the Λ^0/Σ^0 ratio observed at 8 GeV/c [8c]. The $K^-p \to \bar{K}^0 n$ polarization is predicted from the Σ polarization.

Figure 4 Differential cross-section data for $\pi^-p \to \pi^0 n$ (3.8 GeV/c [12a] 4.06 GeV/c [12a]) ; $\pi^-p \to \eta n$ (3.65 GeV/c [13a], 3.7 GeV/c [13b] and 4.0 GeV/c [13c]) and $K_L^0 p \to K_S^0 p$ (4-8 GeV/c spectrum [14]). From the 4 GeV/c interpolations of $\pi^-p \to \pi^0 n$, $K^-p \to \bar{K}^0 n$ and $K^+n \to K^0p$ cross-section data we use the SU(3) sum rule to predict (dashed curve) the $\pi^-p \to \eta^0 n$ data. From the $\pi^-p \to \pi^0 n$ polarization data (3.47 GeV/c [12a] and 5 GeV/c [12b] combined) together with our previous predictions for $K^-p \to \bar{K}^0 n$

and $K^+n \to K^0p$ polarization we similarly predict the $\pi^-p \to \eta n$ polarization near 4 GeV/c (dashed lines). Using the 6 GeV/c $\pi^-p \to \pi^0n$ amplitudes of Ref. 1), our SU(3) predictions for $K_L^0p \to K_S^0p$ cross-section and polarization are shown (dashed). The s channel helicity flip contribution to the cross-section is also shown (dotted).

Figure 5 The bounds on the symmetry breaking factor $|\lambda(t)|^2$ at 4 GeV/c resulting from the cross-section inequality (dashed curves) and the polarized cross-section inequalities (continuous curves).

Figure 6 The bounds on the KN CEX polarizations at 4 GeV/c. The forbidden shaded region follows, on optimizing the triangular inequalities, from the hypercharge exchange data. The dotted region is also forbidden if we assume $|\lambda|^2$ is independent of t and equal to its value at $t = 0$.

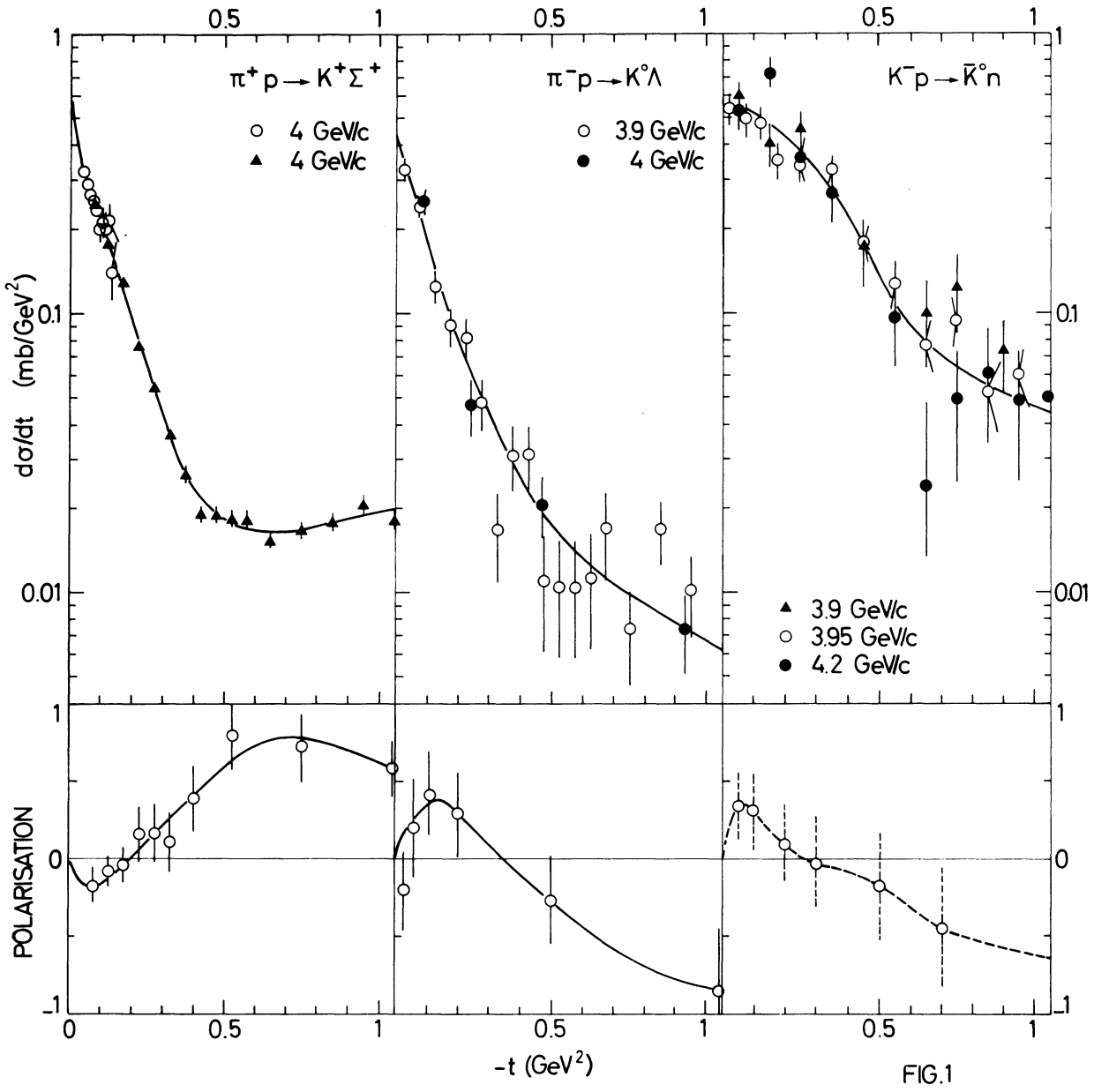
$\pi^+ p \rightarrow K^+ \Sigma^+$
4 GeV/c
4 GeV/c
$\pi^- p \rightarrow K^\circ \Lambda$
3.9 GeV/c
4 GeV/c
$K^- p \rightarrow \bar{K}^\circ n$
3.9 GeV/c
3.95 GeV/c
4.2 GeV/c
dσ/dt (mb/GeV²)
POLARISATION
-t (GeV²)

FIG.1

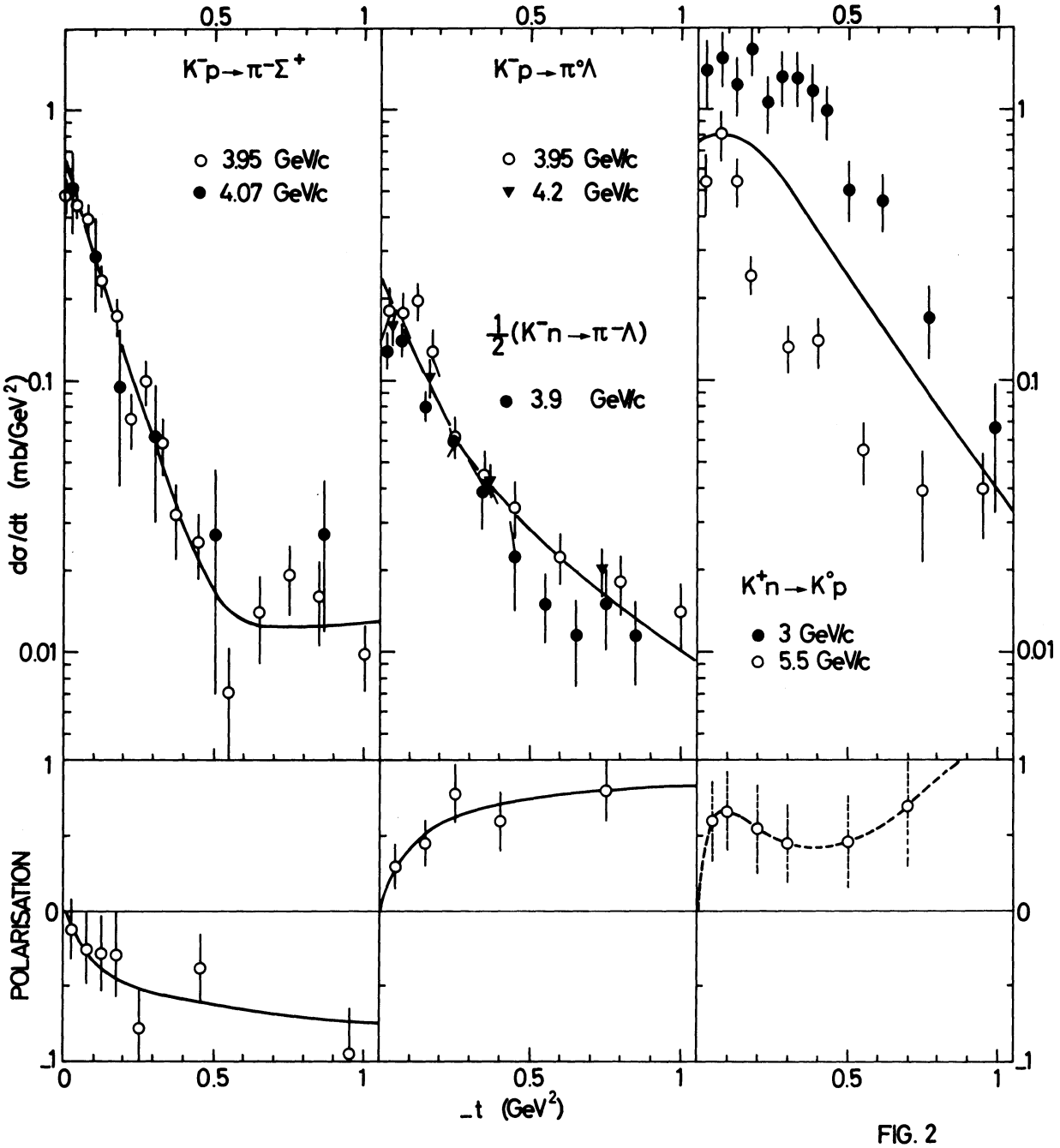
K⁻p → π⁻Σ⁺
○ 3.95 GeV/c
● 4.07 GeV/c
K⁻p → π°Λ
○ 3.95 GeV/c
▼ 4.2 GeV/c
½(K⁻n → π⁻Λ)
● 3.9 GeV/c
K⁺n → K°p
● 3 GeV/c
○ 5.5 GeV/c
dσ/dt (mb/GeV²)
POLARISATION
−t (GeV²)
0.5
1
0.01
0.1
0
−1

FIG. 2

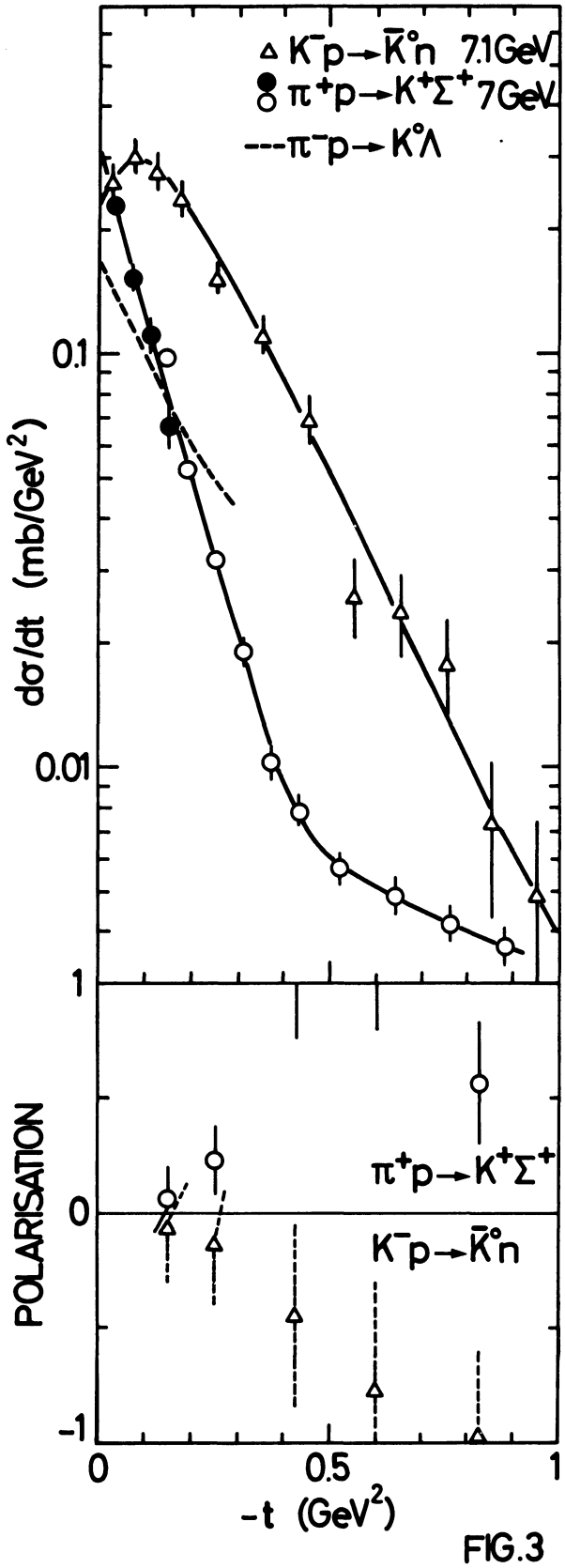
△ K⁻p→K̄°n 7.1GeV
● ○ π⁺p→K⁺Σ⁺ 7GeV
---π⁻p→K°Λ
dσ/dt (mb/GeV²)
0.1
0.01
1
POLARISATION
π⁺p→K⁺Σ⁺
K⁻p→K̄°n
0
-1
0
0.5
1
-t (GeV²)

FIG.3

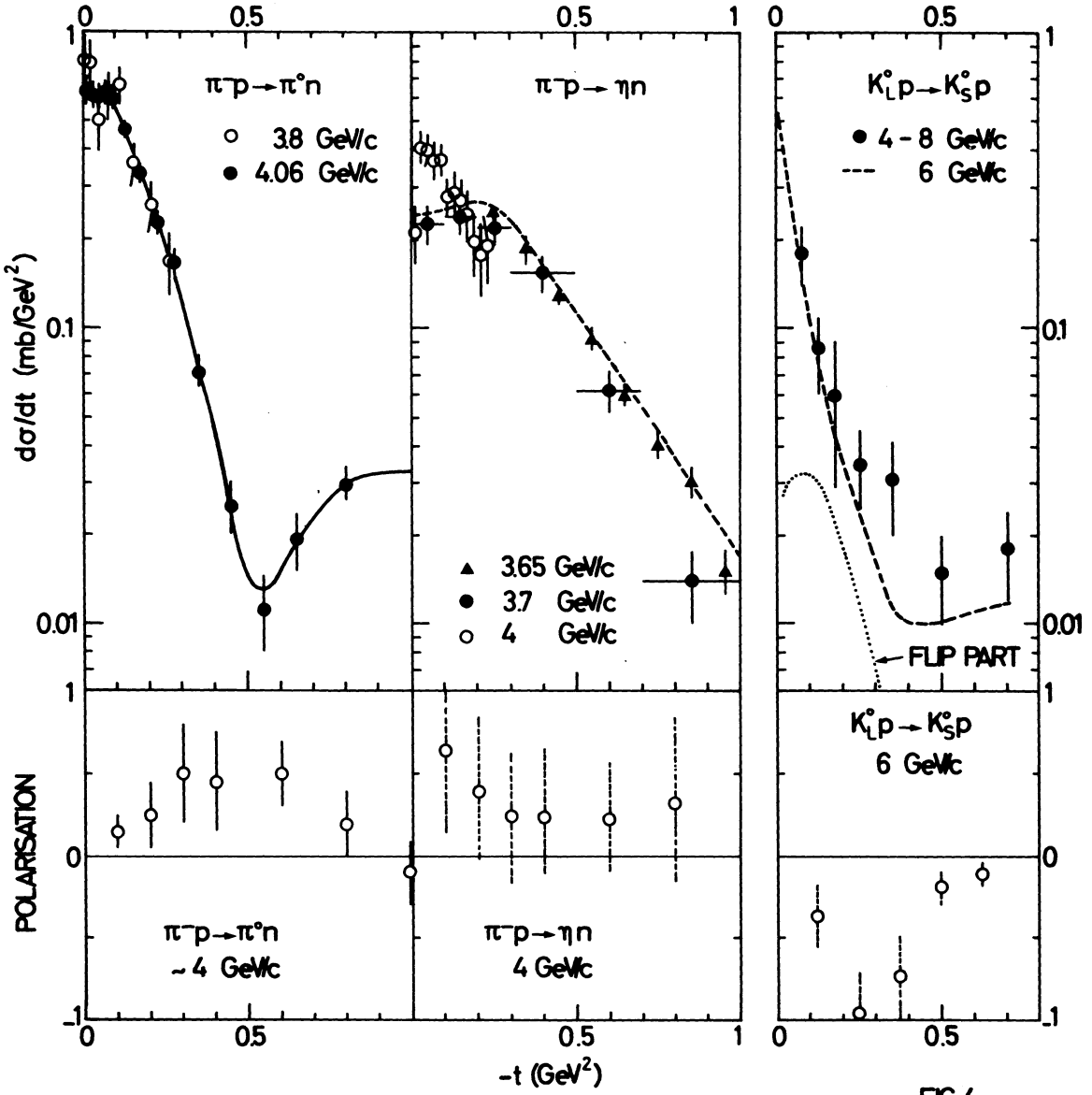
π⁻p→π°n
3.8 GeV/c
4.06 GeV/c
π⁻p→ηn
3.65 GeV/c
3.7 GeV/c
4 GeV/c
K°Lp→K°Sp
4 - 8 GeV/c
6 GeV/c
FLIP PART
dσ/dt (mb/GeV²)
POLARISATION
π⁻p→π°n
~ 4 GeV/c
π⁻p→ηn
4 GeV/c
K°Lp→K°Sp
6 GeV/c
-t (GeV²)

FIG.4

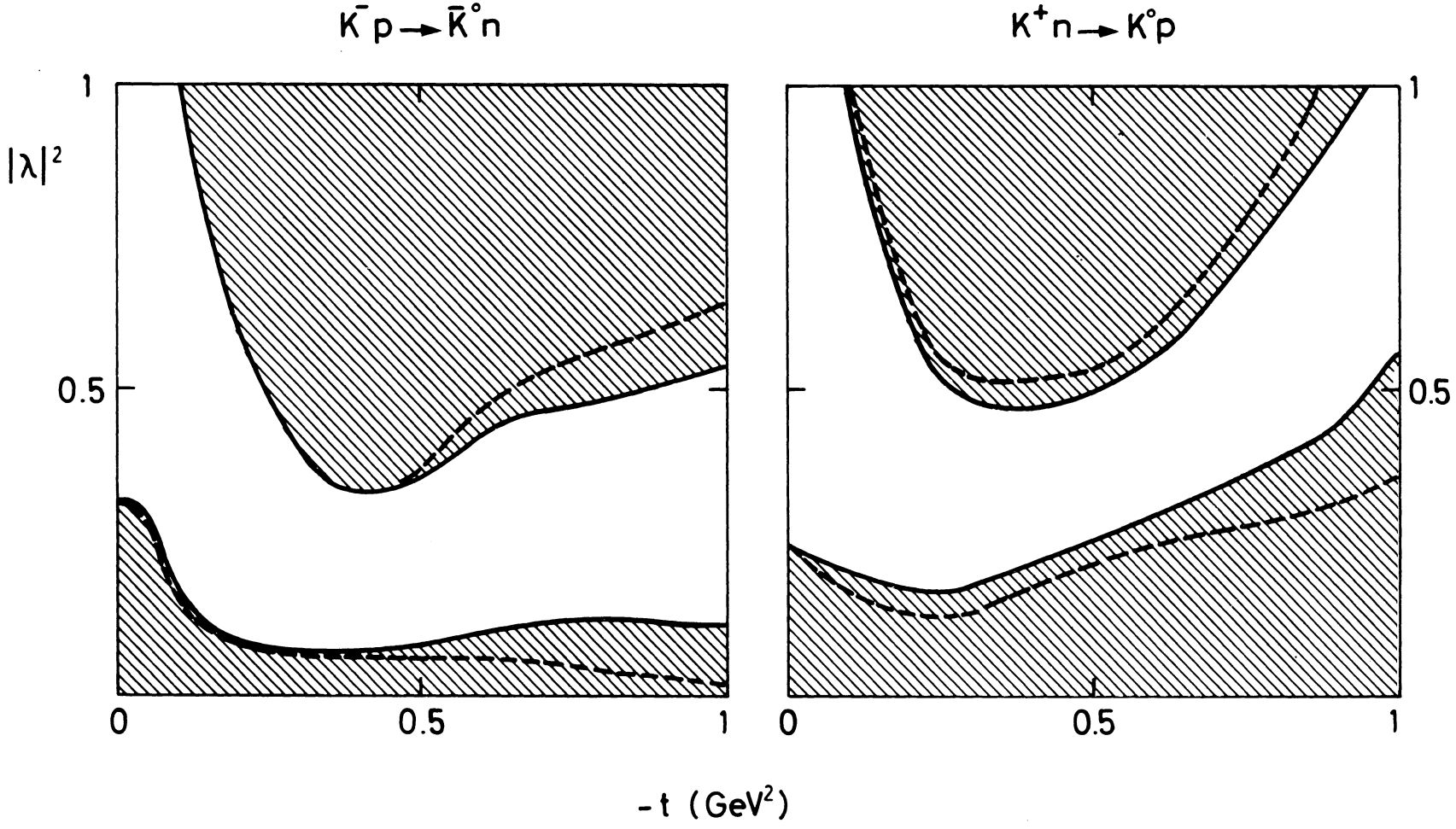

FIG.5

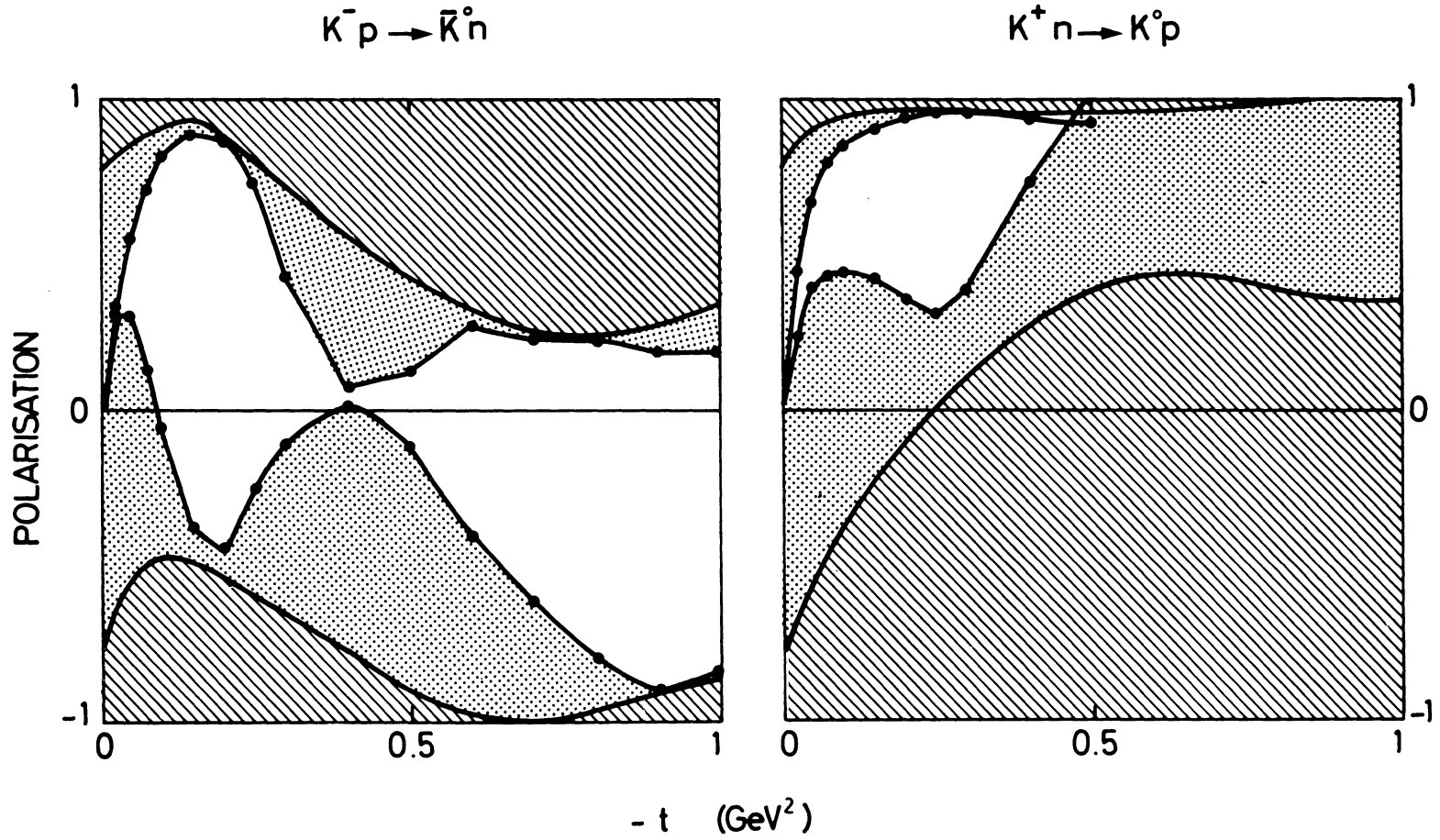
$K^- p \rightarrow \bar{K}^0 n$
$K^+ n \rightarrow K^0 p$
POLARISATION
1
0
-1
0
0.5
1
$-t$ (GeV^2)

FIG.6